Appl. Phys. A 69, 313–321 (1999) / Digital Object Identifier (DOI) 10.1007/s003399900110

Applied Physics A
Materials
Science & Processing

Dopant diffusion and segregation in semiconductor heterostructures: Part III, diffusion of Si into GaAs

C.-H. Chen, U.M. Gösele*, **T.Y. Tan**

Department of Mechanical Engineering and Materials Science, Duke University, Durham, NC 27708-0300, USA
(E-mail: ttan@acpub.dduke.edu)

Received: 19 April 1999/Accepted: 3 May 1999/

Abstract. We have mentioned previously that in the third part of the present series of papers, a variety of n-doping associated phenomena will be treated. Instead, we have decided that this paper, in which the subject treated is diffusion of Si into GaAs, shall be the third paper of the series. This choice is arrived at because this subject is a most relevent heterostructure problem, and also because of space and timing considerations. The main n-type dopant Si in GaAs is amphoteric which may be incorporated as shallow donor species $\mathrm{Si}_{\mathrm{Ga}}^{+}$ and as shallow acceptor species $\mathrm{Si}_{\mathrm{As}}^{-}$. The solubility of $\mathrm{Si}_{\mathrm{As}}^{-}$ is much lower than that of $\mathrm{Si}_{\mathrm{Ga}}^{+}$ except at very high Si concentration levels. Hence, a severe electrical self-compensation occurs at very high Si concentrations. In this study we have modeled the Si distribution process in GaAs by assuming that the diffusing species is $\mathrm{Si}_{\mathrm{Ga}}^{+}$ which will convert into $\mathrm{Si}_{\mathrm{As}}^{-}$ in accordance with their solubilities and that the point defect species governing the diffusion of $\mathrm{Si}_{\mathrm{Ga}}^{+}$ are triply-negatively-charged Ga vacancies V_{Ga}^{3-}. The outstanding features of the Si indiffusion profiles near the Si/GaAs interface have been quantitatively explained for the first time. Deposited on the GaAs crystal surface, the Si source material is a polycrystalline Si layer which may be undoped or n^{+}-doped using As or P. Without the use of an As vapor phase in the ambient, the As- and P-doped source materials effectively render the GaAs crystals into an As-rich composition, which leads to a much more efficient Si indiffusion process than for the case of using undoped source materials which maintains the GaAs crystals in a relatively As-poor condition. The source material and the GaAs crystal together form a heterostructure with its junction influencing the electron distribution in the region, which, in turn, affects the Si indiffusion process prominently.

PACS: 61.72Vv; 61.72Ss; 61.72Yx

The main n-type dopant Si in GaAs is amphoteric, which may be incorporated as shallow donor species $\mathrm{Si}_{\mathrm{Ga}}^{+}$ and as shallow acceptor species $\mathrm{Si}_{\mathrm{As}}^{-}$. The solubility of $\mathrm{Si}_{\mathrm{As}}^{-}$ is much lower than that of $\mathrm{Si}_{\mathrm{Ga}}^{+}$ except at very high Si concentration levels for which a severe electrical self-compensation occurs. The diffusivity of Si in GaAs exhibits a strong dependence on its concentration, which has been modeled by a variety of mechanisms. Greiner and Gibbons [1] assumed that Si diffusion is predominantly carried by SiAs−SiGa pairs. Kavanagh et al. [2] suggested that the concentration dependence is due to a depth-dependent vacancy concentration generated by the Si source material containing As or P. Tan and Gösele [3], Yu et al. [4], and Deppe and Holonyak [5] proposed that the concentration dependence of the Si diffusivity is an effect of the Fermi level, because the point defect species governing Si diffusion in GaAs are the negatively-charged Ga vacancies. To illustrate the principles involved, Deppe and Holonyak [5] considered the singly-negatively-charged Ga vacancies. On the other hand, Yu et al. [4] have quantitatively fitted some of the available experimental data [1, 2] by considering the diffusion of both $\mathrm{Si}_{\mathrm{Ga}}^{+}$ and $\mathrm{Si}_{\mathrm{As}}^{-}$ species. For $\mathrm{Si}_{\mathrm{Ga}}^{+}$, they used mainly the triply-negatively-charged Ga vacancies V_{Ga}^{3-}, and to a lesser extent also the neutral Ga vacancy species V_{Ga}^{0}, as the responsible point defects. For $\mathrm{Si}_{\mathrm{As}}^{-}$, they used the triply-negatively-charged As vacancies V_{As}^{3-} (or self-interstitials I_{As}^{3-}) as the responsible point defect species. In obtaining the fits, V_{Ga}^{3-} is the most important contributor, which is consistent with the fact that V_{Ga}^{3-} also governs Ga self-diffusion and Ga-Al interdiffusion in GaAs/AlAs superlattice under n-doping conditions [6]. Yu et al. [4] also showed that experimental results on Si diffusion into n-type (Sn-doped) GaAs are in contradiction with the Greiner–Gibbons pair-diffusion model [1], and hence it needs not to be further considered. On the other hand, the vacancy injection idea of Kavanagh et al. [2] and the Fermi-level effect are not mutually exclusive on a qualitative basis.

Insofar as V_{Ga}^{3-} dominating the Si diffusion process is concerned, the analysis of Yu et al. [4] appears to be satisfactory. However, Yu et al. [4] used several phenomenological factors in their analysis. First, they invoked the concept of surface states to explain a certain anomalous feature of the Si profiles occurring at the GaAs surface region, which are apparently different quantitatively for the different cases involving

---

[*] Now at: Max-Planck-Institute of Microstructure Physics, Weinberg 2, D-06120 Halle, Germany

different Si source materials and/or different annealing temperatures. Second, partitioning of the Si site occupancy, i.e., the relative concentrations of $\mathrm{Si}_{\mathrm{Ga}}^{+}$ and $\mathrm{Si}_{\mathrm{As}}^{-}$, is arrived at phenomenologically. Third, they have used a single diffusion equation with two effective diffusivities, one for $\mathrm{Si}_{\mathrm{Ga}}^{+}$ and one for $\mathrm{Si}_{\mathrm{As}}^{-}$, to obtain the fits.

Some recent advances allow the above-mentioned aspects to be treated from the point of view of the involved thermodynamic principles instead of just on a phenomenological basis. The first is the development of the diffusion–segregation equation, allowing phenomena of diffusion and segregation to be treated simultaneously [7]. The second is a method of treating the effects on the distribution of charged point defects and dopants associated with semiconductor junctions [8, 9]. The third is a self-consistent calculation of the solubilities of Si on the two GaAs sublattice sites [10]. In this paper we present an analysis of Si indiffusion results [1, 2] by incorporating these advances in the Fermi-level effect model suggested by Yu et al. [4]. Satisfactory fits to these Si indiffusion results were obtained, in particular the anomalous portions of these Si profiles close to the GaAs surface.

1 Formulation

The source material for diffusing Si into GaAs is a polycrystalline Si layer deposited on the surface of the GaAs crystal [1, 2]. The Si-source/GaAs system constitutes a heterostructure. Hence, in modeling the indiffusion process of Si in GaAs, effects of the heterojunction must be accounted for. In the heterojunction region, the electric carrier concentrations are very different from those in the bulk of the semiconductors. The altered carrier concentration in the junction region changes the dopant solubility as well as the concentrations of charged point defects governing dopant atom diffusion in these regions which in turn affect also the dopant distribution behavior in the semiconductor bulk. To formulate the problem mathematically, in the following, we need to consider three aspects: (i) the conversion process of the $\mathrm{Si}_{\mathrm{Ga}}^{+}$ and $\mathrm{Si}_{\mathrm{As}}^{-}$ species; (ii) the diffusion–segregation process of the $\mathrm{Si}_{\mathrm{Ga}}^{+}$ species; and (iii) the carrier diffusion–segregation process in the semiconductor junction region and bulk.

1.1 The conversion process of $\mathrm{Si}_{\mathrm{As}}^{-}$ *and* $\mathrm{Si}_{\mathrm{Ga}}^{+}$

In GaAs the $\mathrm{Si}_{\mathrm{Ga}}^{+}$ and $\mathrm{Si}_{\mathrm{As}}^{-}$ species will convert into each other via the reaction

$$\mathrm{Si}_{\mathrm{Ga}}^{+} + 5\mathrm{e} \Leftrightarrow \mathrm{Si}_{\mathrm{As}}^{-} + V_{\mathrm{Ga}}^{3-} + I_{\mathrm{As}}^{0} , \tag{1}$$

where e is an electron, I_{As}^{0} is the neutral group V element self-interstitials dominating self-diffusion and the diffusion of most impurities dissolved on the group V sublattice sties [11]. In the present analysis we shall assume that the $\mathrm{Si}_{\mathrm{As}}^{-}$ species is not mobile, and hence its concentration change is governed by reaction (1) according to

$$\frac{\partial C_{\mathrm{Si}_{\mathrm{As}}^{-}}}{\partial t} = k_{\mathrm{f}} C_{\mathrm{Si}_{\mathrm{Ga}}^{+}} n^{5} - k_{\mathrm{b}} C_{\mathrm{Si}_{\mathrm{As}}^{-}} C_{V_{\mathrm{Ga}}^{3-}} C_{I_{\mathrm{As}}^{0}} , \tag{2}$$

where C denotes the concentration of the appropriate species, n is the electron concentration, and k_{f} and k_{b} are, respectively, the forward and backward reaction rates in (1). Employing the assumption that a dynamic equilibrium state has been reached for reaction (1), i.e., in (2) the term $\partial C_{\mathrm{Si}_{\mathrm{As}}^{-}}/\partial t$ will be much smaller than either term on its right-hand side (RHS), we obtain

$$\frac{C_{\mathrm{Si}_{\mathrm{As}}^{-}}}{C_{\mathrm{Si}_{\mathrm{Ga}}^{+}}} = k \frac{n^{5}}{C_{V_{\mathrm{Ga}}^{3-}} C_{I_{\mathrm{As}}^{0}}} . \tag{3}$$

The reaction constant k in (3) is given by

$$k = \frac{k_{\mathrm{f}}}{k_{\mathrm{b}}} = \frac{C_{\mathrm{Si}_{\mathrm{As}}^{-}}^{\mathrm{eq}}}{C_{\mathrm{Si}_{\mathrm{Ga}}^{+}}^{\mathrm{eq}}} \frac{C_{V_{\mathrm{Ga}}^{3-}}^{\mathrm{eq}} C_{I_{\mathrm{As}}^{0}}^{\mathrm{eq}}}{n^{5}} , \tag{4}$$

where the superscripts eq denote thermal equilibrium values. Considering that the interface of the Si source material and the GaAs crystal constitutes a perfect sink/source for point defects, $C_{V_{\mathrm{Ga}}^{3-}} = C_{V_{\mathrm{Ga}}^{3-}}^{\mathrm{eq}}$ and $C_{I_{\mathrm{As}}^{0}} = C_{I_{\mathrm{As}}^{0}}^{\mathrm{eq}}$ hold. Therefore, (3) becomes

$$\frac{C_{\mathrm{Si}_{\mathrm{As}}^{-}}}{C_{\mathrm{Si}_{\mathrm{Ga}}^{+}}} = \frac{C_{\mathrm{Si}_{\mathrm{As}}^{-}}^{\mathrm{eq}}}{C_{\mathrm{Si}_{\mathrm{Ga}}^{+}}^{\mathrm{eq}}} = \exp\left(-\frac{g_{\mathrm{Si}_{\mathrm{As}}^{0}}^{\mathrm{eff}} - g_{\mathrm{Si}_{\mathrm{Ga}}^{0}}^{\mathrm{eff}}}{k_{\mathrm{B}} T}\right) \left(\frac{P_{\mathrm{As}_4}}{135 T^{5/2}}\right)^{-1/2} \left(\frac{n}{n_{\mathrm{i}}}\right)^{2} , \tag{5}$$

where the RHS expression obtains from the work of Chen et al. [10]. In (5) k_{B} is Boltzmann's constant, T is the absolute temperature, P_{As_4} is the ambient As_4 vapor pressure which measures the chemical composition of the GaAs crystal, and $g_{\mathrm{Si}_{\mathrm{As}}^{0}}^{\mathrm{eff}}$ and $g_{\mathrm{Si}_{\mathrm{Ga}}^{0}}^{\mathrm{eff}}$ are, respectively, the effective formation Gibbs free energy of the neutral Si atoms on the As and GaAs sites, $\mathrm{Si}_{\mathrm{As}}^{0}$ and $\mathrm{Si}_{\mathrm{Ga}}^{0}$. The RHS of (5) expresses the n dependence of $C_{\mathrm{Si}_{\mathrm{As}}^{-}}/C_{\mathrm{Si}_{\mathrm{Ga}}^{+}}$ explicitly, i.e., the other involved quantities are independent of n.

1.2 The diffusion–segregation process of $\mathrm{Si}_{\mathrm{Ga}}^{+}$

In this study we limit the calculation of Si distribution to within the GaAs crystal. It is assumed that the $\mathrm{Si}_{\mathrm{As}}^{-}$ species is immobile and that the conversion rate of the $\mathrm{Si}_{\mathrm{Ga}}^{+}$ species into the $\mathrm{Si}_{\mathrm{As}}^{-}$ species is small and hence ignorable. Thus, the Si distribution is governed by the simultaneous diffusion–segregation process of $\mathrm{Si}_{\mathrm{Ga}}^{+}$. The segregation process must also be considered because the solubility of $\mathrm{Si}_{\mathrm{Ga}}^{+}$ is dependent upon the semiconductor local n value. The general diffusion–segregation equation discussed by You et al. [7]

$$\frac{\partial C}{\partial t} = \frac{\partial}{\partial x}\left[D\left(\frac{\partial C}{\partial x} - \frac{C}{C^{\mathrm{eq}}}\frac{\partial C^{\mathrm{eq}}}{\partial x}\right)\right] , \tag{6}$$

will be employed to describe the distribution process of $\mathrm{Si}_{\mathrm{Ga}}^{+}$. Equation (6) will also be used to describe the electron distribution process, discussed in Sect. 1.3.

To use (6) for $\mathrm{Si}_{\mathrm{Ga}}^{+}$, note that the second term on the RHS involves $C_{\mathrm{Si}_{\mathrm{Ga}}^{+}}^{\mathrm{eq}}$, which has an implicit dependence on n. This n

dependence is made explicit by the use of [10]

$$C^{\mathrm{eq}}_{\mathrm{Si}^+_{\mathrm{Ga}}} = C^{\mathrm{eq}}_{\mathrm{Si}^0_{\mathrm{Ga}}} \exp\left(\frac{E_{\mathrm{c}} - E_{\mathrm{i}}}{k_{\mathrm{B}} T}\right)\left(\frac{n_{\mathrm{i}}}{n}\right), \tag{7}$$

where E_{c} is the crystal conduction band energy level, E_{i} is the intrinsic Fermi-level, and n_{i} is the intrinsic carrier concentration. In (7) the quantity $C^{\mathrm{eq}}_{\mathrm{Si}^0_{\mathrm{Ga}}}$ is given by

$$C^{\mathrm{eq}}_{\mathrm{Si}^0_{\mathrm{Ga}}} = C_0 \exp\left(-\frac{g^{\mathrm{eff}}_{\mathrm{Si}^0_{\mathrm{Ga}}}}{k_{\mathrm{B}} T}\right)\left(\frac{P_{\mathrm{As}_4}}{135 T^{5/2}}\right)^{-1/2}, \tag{8}$$

where C_0 is the Ga sublattice site density. The use of (7) in (6) yields

$$\frac{\partial C_{\mathrm{Si}^+_{\mathrm{Ga}}}}{\partial t} = \frac{\partial}{\partial x}\left[D_{\mathrm{Si}^+_{\mathrm{Ga}}}\left(\frac{\partial C_{\mathrm{Si}^+_{\mathrm{Ga}}}}{\partial x} - \frac{C_{\mathrm{Si}^+_{\mathrm{Ga}}}}{n_{\mathrm{i}}}\frac{\partial n_{\mathrm{i}}}{\partial x} + \frac{C_{\mathrm{Si}^+_{\mathrm{Ga}}}}{n}\frac{\partial n}{\partial x}\right.\right.$$
$$\left.\left. - \frac{C_{\mathrm{Si}^+_{\mathrm{Ga}}}}{C_{\mathrm{Si}^0_{\mathrm{Ga}}}}\frac{\partial C_{\mathrm{Si}^0_{\mathrm{Ga}}}}{\partial x} - \frac{C_{\mathrm{Si}^0_{\mathrm{Ga}}}}{2 k_{\mathrm{B}} T}\frac{\partial (E_{\mathrm{c}} - E_{\mathrm{i}})}{\partial x}\right)\right], \tag{9}$$

where $D_{\mathrm{Si}^+_{\mathrm{Ga}}}$ is the diffusivity of the $\mathrm{Si}^+_{\mathrm{Ga}}$ species. In accordance with the conclusion of Yu et al. [4], we assume that the diffusion of $\mathrm{Si}^+_{\mathrm{Ga}}$ is governed by V^{3-}_{Ga}. Hence,

$$D_{\mathrm{Si}^+_{\mathrm{Ga}}} = D_{\mathrm{Si}^+_{\mathrm{Ga}}}(n_{\mathrm{i}})\left(\frac{n}{n_{\mathrm{i}}}\right)^3, \tag{10}$$

where $D_{\mathrm{Si}^+_{\mathrm{Ga}}}(n_{\mathrm{i}})$ is the diffusivity of $\mathrm{Si}^+_{\mathrm{Ga}}$ under intrinsic conditions.

1.3 Electron distribution

In contrast to the distribution of Si, the distribution of electrons will be calculated throughout the heterostructure, i.e., the electron distribution in the Si source materials will also be included. The distribution of electrons is obtained also using (6). The electron concentration in the heterostructure under thermal equilibrium conditions is given by

$$n^{\mathrm{eq}} = N_{\mathrm{c}} \exp\left(\frac{E^{\mathrm{eq}}_{\mathrm{F}} - E_{\mathrm{c}} + q\phi}{k_{\mathrm{B}} T}\right), \tag{11}$$

where N_{c} is the conduction band effective density of states of each of the semiconductors forming the heterostructure, $E^{\mathrm{eq}}_{\mathrm{F}}$ is an appropriate Fermi-level which is constant throughout the heterostructure, E_{c} refers to that of each semiconductor without band bending or shifting, q is the charge of an electron (taken to be positive), and ϕ is the electrostatic potential satisfying Poisson's equation

$$\frac{\mathrm{d}^2\phi}{\mathrm{d}x^2} = \frac{-q}{\varepsilon_{\mathrm{s}}}\left(N^+_{\mathrm{D}} + p - n - N^-_{\mathrm{A}}\right), \tag{12}$$

where ε_{s} is the semiconductor dielectric constant, p is the hole concentration which is equal to n^2_{i}/n. The quantities N^+_{D} and N^-_{A} are, respectively, the total ionized donor and acceptor concentrations in each of the semiconductors forming the heterostructure: $N^+_{\mathrm{D}} = C_{\mathrm{Si}^+_{\mathrm{Ga}}}$ and $N^-_{\mathrm{A}} = C_{\mathrm{Si}^-_{\mathrm{As}}}$ in GaAs, while $N^+_{\mathrm{D}} = 0$, or C_{P^+}, or C_{As^+} and $N^-_{\mathrm{A}} = 0$ in Si.

Under Si indiffusion conditions, n is a function of both t and x. Using (11) in (6), the distribution process of n is described by

$$\frac{\partial n}{\partial t} = \frac{\partial}{\partial x}\left[D_{\mathrm{n}}\left(\frac{\partial n}{\partial x} - \frac{n}{N_{\mathrm{c}}}\frac{\partial N_{\mathrm{c}}}{\partial x} + \frac{n}{k_{\mathrm{B}} T}\frac{\partial E_{\mathrm{c}}}{\partial x} - \frac{qn}{k_{\mathrm{B}} T}\frac{\partial \phi}{\partial x}\right)\right], \tag{13}$$

where D_{n} is the electron diffusivity.

2 Analyses of experimental data

Equation (5), (9), (12), and (13) are solved numerically using the general purpose partial differential equation solver ZOMBIE [12] to obtain fits to the available experimental data [1,2]. These experimental data include undoped Si source material cases [1,2] as well as cases of using n-doped Si source materials doped by either As or P [2].

Equations (12) and (13) are solved to obtain the electron distribution throughout the involved heterostructure including the GaAs crystal and the Si source material. In order to avoid the complexities associated with treating Si self-diffusion in the Si source material, however, (9) is solved to obtain the Si distribution only in the GaAs crystal. This is carried out by using the value of $C_{\mathrm{Si}^-_{\mathrm{As}}}/C_{\mathrm{Si}^+_{\mathrm{Ga}}}$ according to (5) at the interface on the GaAs side as a boundary condition for solving (9). In accordance with Chen et al. [10], the value of $g^{\mathrm{eff}}_{\mathrm{Si}^0_{\mathrm{As}}} - g^{\mathrm{eff}}_{\mathrm{Si}^0_{\mathrm{Ga}}}$ in (5) is taken to be 1.6 eV. The P_{As_4} value used in (5) for the different cases will be mentioned together with the analytical results.

Figure 1a shows our fits of the experimental data of Greiner and Gibbons [1] on diffusing Si into GaAs, including the total Si and electron concentrations, and Fig. 1b shows our calculated total Si concentration and the concentrations of the $\mathrm{Si}^+_{\mathrm{Ga}}$ and $\mathrm{Si}^-_{\mathrm{As}}$ species. These data (and fits) clearly demonstrated the amphoteric nature of Si in GaAs, particularly that the difference in the C_{Si} and n values in the GaAs crystal bulk shown in Fig. 1a results from electrical self-compensation of the two species, i.e., $n \approx C_{\mathrm{Si}^+_{\mathrm{Ga}}} - C_{\mathrm{Si}^-_{\mathrm{As}}}$. In the experiment, the source material is an undoped Si layer capped by a SiO_2 layer. The samples were annealed at 1050 °C for 3 s in an ambient rich in As vapor, which we took as $P_{\mathrm{As}_4} = 1$ atm. Table 1 lists the other materials' constants used, including $D_{\mathrm{Si}^+_{\mathrm{Ga}}}(n_{\mathrm{i}})$, n_{i}, E_{c}, and E_{i}, with the values of E_{c} and E_{i} also applying to other cases discussed below. The listed energetic values are those at room temperature, with the zero of energy referring to that of the vacuum level. The high-temperature values of these constants are not known from the literature and there is also a lacking of required information for extrapolating these values to high temperatures.

Figure 2 shows our fit of the experimental data of Kavanagh et al. [2] on diffusing Si into GaAs from an undoped polycrystalline Si source material at 1050 °C for 10 s. The P_{As_4} value used in (5) for this case is 10^{-4} atm. Also shown in Fig. 2 are our fits to the data of Kavanagh et al. [2] on diffusing Si into GaAs from As-doped polycrystalline Si source materials at 940 to 1000 °C for 10 s. For the As-doped source cases, there are no data or fits for a depth of less than

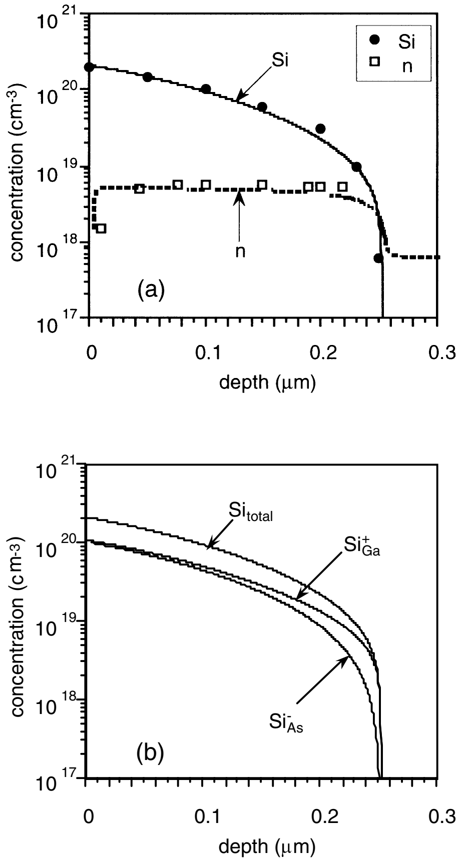

Fig. 1. **a** The electron and total Si concentration data of Greiner and Gibbons [1] together with the calculated fitting curves. **b** The calculated total Si concentration and the concentrations of the $\mathrm{Si}^+_{\mathrm{Ga}}$ and $\mathrm{Si}^-_{\mathrm{As}}$ species

20 nm. In the experiments [2] it was found that As precipitates formed in surface layers to the depth of 20 nm. Hence only data beyond this depth were reported, and in our calculations we have taken the Si/GaAs interface to be at the depth of 20 nm. For these cases the Si source materials are n^+-type due to doping by As. The As concentration is 12 at. %, which exceeded the As solid solubility values at the appropriate experimental temperatures. In obtaining the present fits, we have used the appropriate As solid solubility values [13] at the experimental temperatures and computed the corresponding electron solubility values using charge neutrality conditions, which are listed in Table 2. The P_{As_4} value used in (5) for the As-doped source case is 10 atm, since it is judged that the As atoms in the Si source material will render the GaAs crystal to be As-rich.

Table 1. Values of materials constants used for obtaining fit of the 1050 °C data of Greiner and Gibbons [1]. The E_c and E_i values apply also to other cases

	E_c /eV	E_i /eV	n_i cm^{-3}	$D_{\mathrm{Si}^+_{\mathrm{Ga}}}$ (n_i) cm^{2}s^{-1}
Si	−4.04	−4.59	7×10^{18}	
GaAs	−4.07	−4.77	7×10^{17}	7×10^{-14}

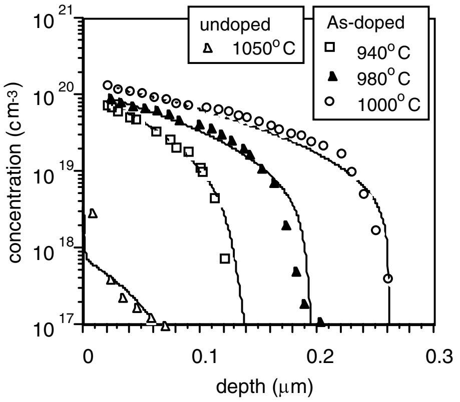

Fig. 2. The Si concentration data of Kavanagh et al. [2] obtained using undoped and As-doped Si source materials together with the calculated fitting curves

Figure 3 shows our fits to the experimental data of Kavanagh et al. [2] on diffusing Si into GaAs from P-doped polycrystalline Si source materials at 900 to 1020 °C for 10 s. These Si source materials are n^+-type due to doping by P. The P concentration is 20 at. %, which exceeded the P solubility limits at the appropriate temperatures. In obtaining the present fits, the used P solid solubility and the corresponding electron solubility values are listed in Table 3. The P_{As_4} value used in (5) for these cases is also 10 atm, since the P atoms in the Si source material will also effectively render the GaAs crystal to be As-rich. Due to P indiffusion into GaAs during annealing, a thin surface layer of GaAs turned into $\mathrm{GaP}_y\mathrm{As}_{1-y}$ materials with a variable y value. Thus, the structure contains an abrupt junction and a continuous transition layer of $\mathrm{Si/GaP}_y\mathrm{As}_{1-y}$. The presence of the $\mathrm{GaP}_y\mathrm{As}_{1-y}$ material renders the analysis considerably more complicated, for several reasons. First, formation of $\mathrm{GaP}_y\mathrm{As}_{1-y}$ is time dependent. Second, the $\mathrm{GaP}_y\mathrm{As}_{1-y}$ band structure is dependent upon y, i.e., E_g, E_c, E_v, and E_i are all functions of y. Third, the band structure dependence of y leads also to varying Si solubility values in the $\mathrm{GaP}_y\mathrm{As}_{1-y}$ layer. These aspects are treated as follows. First, based on the observation that the P concentration in $\mathrm{GaP}_y\mathrm{As}_{1-y}$ follows a complementary error function [2], formation of the $\mathrm{GaP}_y\mathrm{As}_{1-y}$ layer has been modeled by

$$\frac{\partial C_P}{\partial t} = \frac{\partial}{\partial x}\left(D_P \frac{\partial C_P}{\partial x}\right), \tag{14}$$

where C_P and D_P are, respectively, the concentration and diffusivity of P. The used values of D_P and C_P at the surface are chosen in accordance with the experimental results of Kavanagh et al. [2], see Table 4, which also includes the range of y values in each experiment. Second, it is known [14] that for $y < 0.425$, $\mathrm{GaP}_y\mathrm{As}_{1-y}$ is a direct band gap material with the conduction band edge energy determined by that of the X band, whereas for $y > 0.425$, $\mathrm{GaP}_y\mathrm{As}_{1-y}$ becomes an indirect band gap material with the conduction band edge energy determined by that of the Γ band. According to Cappizi et al. [14], the $\mathrm{GaP}_y\mathrm{As}_{1-y}$ band structure related energy values are given by

$$E_g(\mathrm{GaP}_y\mathrm{As}_{1-y}) = 1.515 + 1.172y + 0.186y^2\,\mathrm{eV}, \quad 0 \le y \le 0.425 \tag{15a}$$

$$E_g(\mathrm{GaP}_y\mathrm{As}_{1-y}) = 1.9715 + 0.144y + 0.211y^2\,\mathrm{eV}, \quad 0.425 \le y \le 1 \tag{15b}$$

Table 2. Values of materials constants used for obtaining fits of the data of Kavanagh et al. [1] obtained using undoped and As-doped Si source materials

T /°C	n_i in GaAs /cm^{-3}	$D_{\mathrm{Si}_{\mathrm{Ga}}^{+}}(n_i)$ /cm^{2}s^{-1}	n_i in Si /cm^{-3}	As solid solubility in Si /cm^{-3}	n in As-doped Si /cm^{-3}
			undoped Si source materials		
1050	7×10^{17}	1.1×10^{-15}	7×10^{18}		
			As-doped Si source materials		
940	3×10^{17}	1.55×10^{-15}	4×10^{18}	1.2×10^{21}	1.59×10^{20}
980	3.78×10^{17}	5.8×10^{-15}	4.12×10^{18}	1.34×10^{21}	2.014×10^{20}
1000	4.53×10^{17}	1.15×10^{-14}	5×10^{18}	1.41×10^{21}	2.12×10^{20}

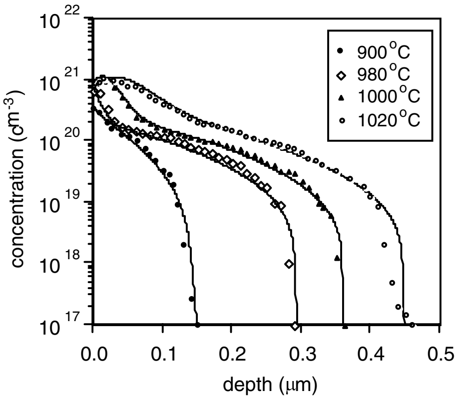

Fig. 3. The Si concentration data of Kavanagh et al. [2] obtained using P-doped Si source materials together with the calculated fitting curves

Table 4. Values of the maximum P concentration (C_{P}) in GaP$_y$As$_{1-y}$, the y value range, and the P diffusivity (D_{P}) in GaP$_y$As$_{1-y}$/GaAs used for calculating fits for the experimental data of Kavanagh et al. [1] obtained using P-doped Si source materials

T /°C	C_{P} /cm^{-3}	y range	D_{P} /cm^{2}s^{-1}
900	1.6×10^{21}	0–0.072	1×10^{-13}
980	6.6×10^{21}	0–0.296	3×10^{-13}
1000	1.54×10^{22}	0–0.691	7×10^{-13}
1020	1.54×10^{22}	0–0.691	1.2×10^{-12}

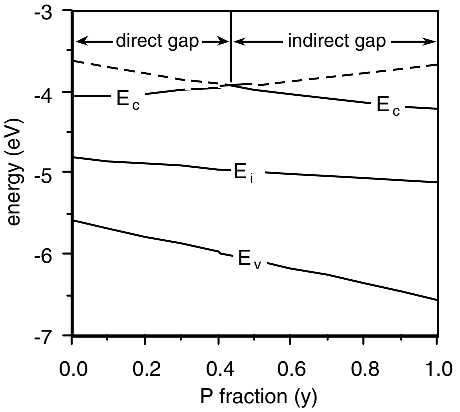

Fig. 4. Values of E_c, E_i, and E_v of the material GaP$_y$As$_{1-y}$ as a function of the group V element composition y

for the band gap;

$$E_c(\mathrm{GaP}_y\mathrm{As}_{1-y}) = -4.07 + 0.207y + 0.186y^2\,\mathrm{eV}, \quad 0 \le y \le 0.425 \tag{16a}$$

$$E_c(\mathrm{GaP}_y\mathrm{As}_{1-y}) = -3.6135 - 0.821y + 0.211y^2\,\mathrm{eV}, \quad 0.425 \le y \le 1 \tag{16b}$$

for E_c;

$$E_V(\mathrm{GaP}_y\mathrm{As}_{1-y}) = -5.585 - 0.965y\,\mathrm{eV} \tag{17}$$

for E_V; and

$$E_i(\mathrm{GaP}_y\mathrm{As}_{1-y}) = -4.81 - 0.38y + 0.09y^2\,\mathrm{eV} \tag{18}$$

for E_i. The band structure of the GaAs$_y$P$_{1-y}$ material as a function of y is shown in Fig. 4. Third, assuming that the solubilities of the neutral Si atoms on both the group III and group V sublattices are the same in the GaAs$_y$P$_{1-y}$ materials and in GaAs, and that n_i/n is also the same, then the $\mathrm{Si}_{\mathrm{Ga}}^{+}$ solubility difference between existing in GaAs$_y$P$_{1-y}$ and in GaAs materials will be only due to the band structure variations. That is, according to (7),

$$\frac{C_{\mathrm{Si}_{\mathrm{Ga}}^{+}}(\mathrm{GaP}_y\mathrm{As}_{1-y})}{C_{\mathrm{Si}_{\mathrm{Ga}}^{+}}(\mathrm{GaAs})} = \frac{\exp\left(\frac{E_c(\mathrm{GaP}_y\mathrm{As}_{1-y}) - E_i(\mathrm{GaP}_y\mathrm{As}_{1-y})}{k_B T}\right)}{\exp\left(\frac{E_c(\mathrm{GaAs}) - E_i(\mathrm{GaAs})}{k_B T}\right)} \tag{19}$$

holds. The value of $E_c - E_i$ is not a constant in the GaP$_y$As$_{1-y}$ layer because of its band structure dependence on y while the value of y changes in this material layer. The band gap of GaP$_y$As$_{1-y}$ (the $E_c - E_i$ value) is larger than that of GaAs

Table 3. Values of materials constants used for obtaining fits of the data of Kavanagh et al. [1] obtained using P-doped Si source materials

T /°C	n_i in GaAs /cm^{-3}	$D_{\mathrm{Si}_{\mathrm{Ga}}^{+}}(n_i)$ /cm^{2}s^{-1}	n_i in Si /cm^{-3}	P solid solubility in Si /cm^{-3}	n in P-doped Si /cm^{-3}
900	2×10^{17}	1.55×10^{-16}	2.2×10^{18}	6×10^{20}	8.8×10^{19}
980	3.78×10^{17}	4.3×10^{-15}	4.12×10^{18}	9.7×10^{20}	1.02×10^{20}
1000	4.53×10^{17}	1.1×10^{-14}	5×10^{18}	1×10^{21}	1.1×10^{20}
1020	6×10^{17}	2.6×10^{-14}	6.5×10^{18}	1.12×10^{21}	1.32×10^{20}

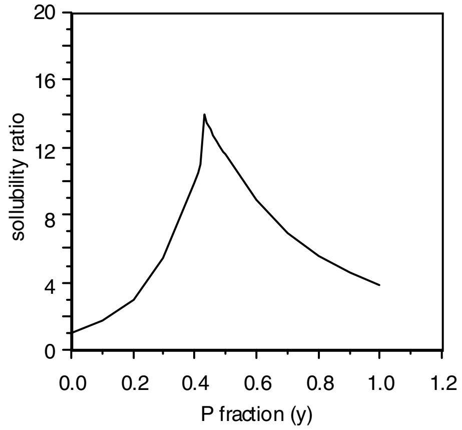

Fig. 5. Solubility ratio of $\mathrm{Si}_{\mathrm{Ga}}^{+}$ in $\mathrm{GaP}_y\mathrm{As}_{1-y}$ and in GaAs as a function of y at 1000 °C, under conditions that the solubilities of the $\mathrm{Si}_{\mathrm{Ga}}^{0}$ are the same in both materials and that the values of n_{i}/n are also the same in both materials

for $y > 0$. Thus, according to (19), the $\mathrm{Si}_{\mathrm{Ga}}^{+}$ solubility in $\mathrm{GaP}_y\mathrm{As}_{1-y}$ will be larger than that in GaAs under the conditions that $C_{\mathrm{Si}_{\mathrm{Ga}}^{0}}^{\mathrm{eq}}$ and (n_{i}/n) are the same in both materials. Figure 5 shows the value of (19) at 1000 °C.

3 Discussions

Although Si is the main n-type dopant in GaAs, regarding the involved Si diffusion mechanisms, both useful experimental data and interpretations are limited. The most outstanding experimental features are that the Si diffusivity appears to be highly concentration dependent [1, 2], and that the use of n-doped Si source materials is much more effective in diffusing Si into GaAs [2]. Greiner and Gibbons [1] interpreted their experimental result by invoking a SiGa−SiAs pair diffusion model, which, however, has been found to be in contradiction with results of diffusing Si into Sn-doped n-type GaAs [4]. Kavanagh et al. [2] observed outdiffusion of Ga atoms from GaAs into the As- and P-doped Si source materials to form GaAs or GaP materials. This led to their V_{Ga} injection model for explaining the results: the As- and P-doped source materials are more effective because diffusion of Ga atoms out of GaAs injects V_{Ga} into the GaAs crystal more effectively than in the case of using undoped Si materials. They further suggested that the Si diffusivity is concentration dependent because the injected V_{Ga} species have a concentration gradient. On the other hand, Yu et al. [4] identified V_{Ga}^{3-} as the point defect species governing $\mathrm{Si}_{\mathrm{Ga}}^{+}$ diffusion in GaAs. Their model contains phenomenological aspects for which the underlying physical causes are identified in the present study.

In the present study we have adopted the V_{Ga}^{3-} model of Yu et al. and recognized that the Si source materials and GaAs form heterostructures, which are associated with several effects. First, the source material influences the chemical composition of the GaAs crystals. For the data of Kavanagh et al. [2], for which no ambient As vapor phase materials were used, the As- or P-doped source materials effectively rendered the GaAs crystals into an As-rich composition with a needed P_{As_4} value of 10 atm for obtaining the fits, while for the case of using undoped Si source the GaAs crystal composition is that under an As-poor condition for which the needed P_{As_4} value is 10^{-4} atm. In the case of Greiner and Gibbons [1], in which the Si source material is undoped but an As vapor phase was present in the ambient, the needed P_{As_4} value is 1 atm. For the two undoped Si source material cases [1, 2], the difference between the needed P_{As_4} values is apparently due to the GaAs crystal initial composition difference and the use of an ambient As vapor phase in the experiment or not. The difference in P_{As_4} values in the different cases means that the thermal equilibrium concentrations of the V_{Ga}^{3-} species, which governs $\mathrm{Si}_{\mathrm{Ga}}^{+}$ diffusion, are different, and hence also are the $\mathrm{Si}_{\mathrm{Ga}}^{+}$ diffusivity values. Figure 6 shows the $D_{\mathrm{Si}_{\mathrm{Ga}}^{+}}(n_{\mathrm{i}})$ values used in obtaining the fits for all cases. In Fig. 6 the $D_{\mathrm{Si}_{\mathrm{Ga}}^{+}}(n_{\mathrm{i}})$ values for the As-rich GaAs crystal cases are fitted by

$$D_{\mathrm{Si}_{\mathrm{Ga}}^{+}}(n_{\mathrm{i}}) = 5.2 \times 10^{5} \exp\left(-\frac{4.98\,\mathrm{eV}}{k_{\mathrm{B}}T}\right) \mathrm{cm}^{2}\mathrm{s}^{-1}\,, \tag{20}$$

which is lager than that given by Yu et al. [4] by a factor of 10. For the data of Kavanagh et al. [2], the $D_{\mathrm{Si}_{\mathrm{Ga}}^{+}}(n_{\mathrm{i}})$ values of the doped source cases are larger than that of the undoped source case by a factor of ≈ 18. Since in the present study $\mathrm{Si}_{\mathrm{Ga}}^{+}$ diffusion in GaAs is assumed to be governed by V_{Ga}^{3-}, we have $D_{\mathrm{Si}_{\mathrm{Ga}}^{+}}(n_{\mathrm{i}}) \alpha C_{V_{\mathrm{Ga}}^{3-}}^{\mathrm{eq}}(n_{\mathrm{i}}) \alpha P_{\mathrm{As}_4}^{1/4}$ holding, where $C_{V_{\mathrm{Ga}}^{3-}}^{\mathrm{eq}}(n_{\mathrm{i}})$ is the thermal equilibrium concentration of V_{Ga}^{3-} under intrinsic conditions. This is consistent with the ratio $(10/10^{-4})^{1/4} = 17.8$ for the $P_{\mathrm{As}_4}^{1/4}$ dependence of $D_{\mathrm{Si}_{\mathrm{Ga}}^{+}}(n_{\mathrm{i}})$ between the doped and undoped Si source cases of Kavanagh et al. [2]. In the interpretations of Kavanagh et al. [2] and in ours, the mechanisms for the concentration value of the point defects has a similarity. In the interpretation of Kavanagh et al. [2], P or As causes V_{Ga} injection in abundance, whereas in our interpretation they cause the GaAs crystal to be rich in As, resulting in a higher V_{Ga} concentration. In our interpretation, it cannot be assumed that the GaAs crystals are initially As-rich, and hence must become As-rich due to rapid injection of V_{Ga}. Thus, V_{Ga} injection is a common feature in both interpretations. However, the mechanisms responsible for the V_{Ga} concentration gradients are very different in the two interpretations. In the interpretation of Kavanagh et al. [2] this results

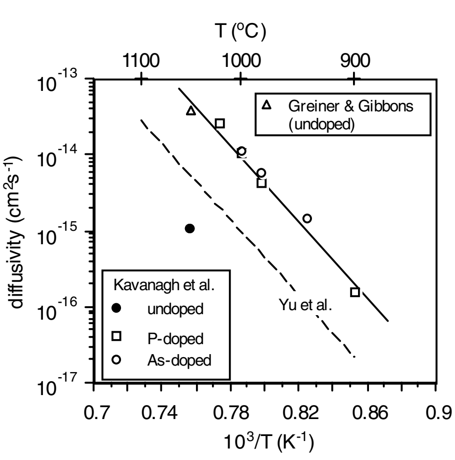

Fig. 6. The $\mathrm{Si}_{\mathrm{Ga}}^{+}$ diffusivity values under intrinsic conditions, $D_{\mathrm{Si}_{\mathrm{Ga}}^{-}}(n_{\mathrm{i}})$, used for obtaining fits for all cases

from the low V_{Ga} migration rate which leads to a non-steady-state V_{Ga} distribution. In our interpretation the concentrations gradient is due to the Fermi-level effect, with V_{Ga}^{3-} being in thermal equilibrium with the local n value, while the V_{Ga}^{0} concentration is the thermal equilibrium value. This requires the V_{Ga}^{3-} diffusion rate to be much higher than that of Si.

In this study it has been recognized that the Si source material and the GaAs crystal together constitute a semiconductor heterostructure. The heterojunction determines the electrical carrier distribution in the junction region which in turn affects the distribution of ionized dopant atoms and charged point defects governing the diffusion of the dopant atoms in the region and beyond.

It is seen from Fig. 1 that the calculated n values dip down at the Si/GaAs interface, indicating that electrons in GaAs are depleted at the heterojunction. In Fig. 7a, wherein the calculated experimental temperature (1050 °C) electron distribution across the heterojunction is plotted with the depth scale expanded, it is clearly seen that electrons are depleted on the GaAs side and accumulated on the Si side. From the corresponding band structure shown in Fig. 7b, it is seen that this electron depletion/accumulation phenomena results from the fact that the GaAs crystal is n-type with a Fermi-level above that of a separate undoped Si crystal at 1050 °C. Consequently, in the heterostructure depletion and accumulation of electrons develop, respectively, on the GaAs side and the Si side of the heterojunction. It is seen from Fig. 7a that, at 1050 °C the intrinsic electron concentration n_{i} in the Si bulk is actually higher than the n value in the GaAs bulk, but, under thermal equilibrium conditions, electrons have flown from GaAs to Si in the junction region. This is because the driving force is the Fermi-level or chemical potential of electrons, which is higher in GaAs than in a separate Si crystal. The depletion of electrons on the GaAs side of the junction reduces the effectiveness of diffusing Si into GaAs, because the lower n value maintains the junction region thermal equilibrium concentration of V_{Ga}^{3-} at a much lower value than that in the GaAs bulk, which means that the $\text{Si}_{\text{Ga}}^{+}$ flux flowing into the GaAs crystal bulk will be correspondingly smaller. In Fig. 1, the n value data of Greiner and Gibbons at the junction is also smaller than those in the bulk. This is, however, probably a fortuitous coincidence, since in measuring the n values at room temperature using the Van der Pauw method, the Si layer should have been stripped away.

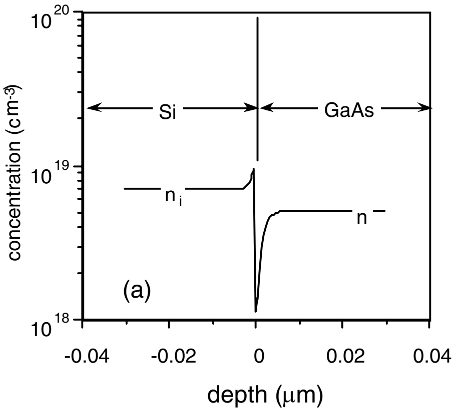

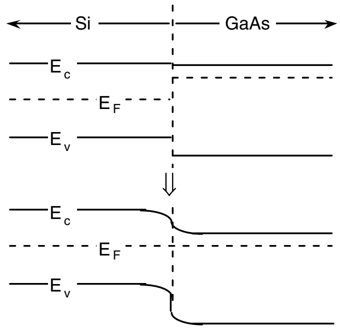

(b)

Fig. 7. a Calculated electron distribution in Si and in GaAs for the case of Greiner and Gibbons [1], drawn in expanded depth scale for showing electron accumulation in the Si source material and electron depletion in GaAs across the heterojunction. **b** The corresponding band diagram. The *upper panel* is for the individual Si and GaAs crystals and the *lower panel* is for the same materials forming the heterostructure

Figure 8 shows the calculated experimental temperature n values for the cases of Kavanagh et al. using As-doped Si source materials [2], for which there is no reported experimental data. In contrast to the undoped Si source cases, the n values at the Si/GaAs interface indicate that electrons are accumulated on the GaAs side. In Fig. 8 the heterojunction is taken to be at the 20 nm position, in both the experimental data and in our calculated fits, because within this depth As precipitation has occurred [2]. The electron accumulation phenomena is clearly seen by the example shown in Fig. 9a wherein the depth scale is expanded and the calculated n values are across the heterojunction, with its position now marked zero. In As-doped cases the Si source materials are n^{+}-type with a Fermi-level above E_{c} due to degenerate doping, while the GaAs crystal is n-type. Thus, the Fermi-level of Si is higher than that of a separate GaAs crystal, and in the heterostructure electrons are accumulated on the GaAs side and depleted on the Si side of the heterojunction. The corresponding band diagram is shown in Fig. 9b. The accumulated electrons on the GaAs crystal junction region enhance the effectiveness of diffusing Si into GaAs, because the higher n value will enhance the thermal equilibrium concentration of V_{Ga}^{3-} to a value much higher than that in the GaAs bulk at the

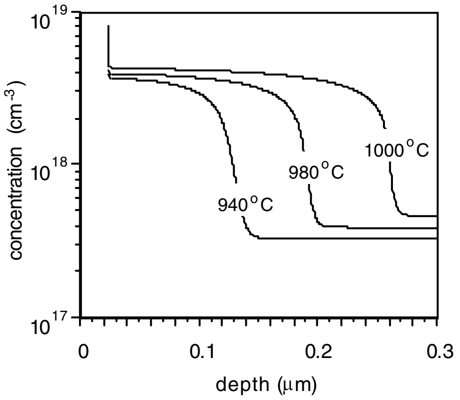

Fig. 8. Calculated experimental temperature electron distributions in Si and in GaAs for the As-doped Si source material cases of Kavanagh et al. [2]

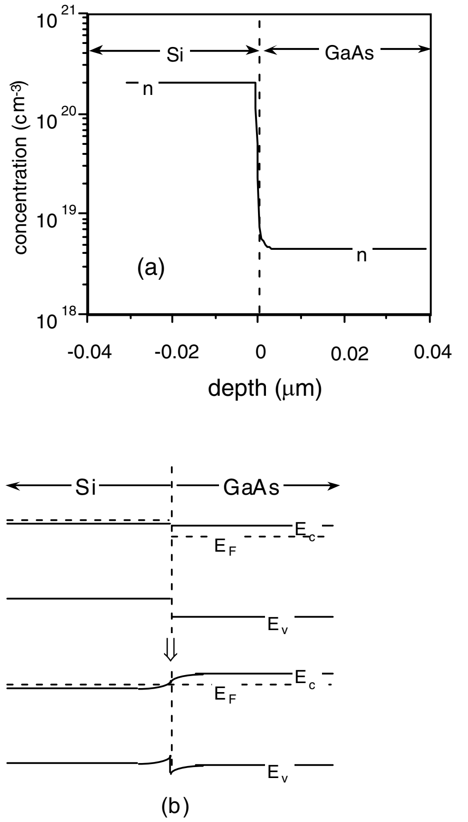

Fig. 9. **a** Calculated electron distribution at 1000 °C in Si and GaAs for the As-doped Si source material case of Kavanagh et al. [2], drawn in expanded depth scale for showing electron depletion in the Si source material and electron accumulation in GaAs across the heterojunction. **b** The corresponding band diagram. The *upper panel* is for individual Si and GaAs crystals and the *lower panel* is for the same materials forming the heterostructure

same doping level, which means that the $\mathrm{Si}_{\mathrm{Ga}}^{+}$ flux flowing into the GaAs crystal bulk will be correspondingly larger.

The P-doped Si source cases, for which $\mathrm{GaP}_y\mathrm{As}_{1-y}$ materials formed, are more complicated in that the Si profiles possess features not present in those of the other cases. Near the junction to a considerable depth, the profile is concave upward for the two lower temperature cases, while the same profile portion is of a shape of an upward convex bulge for the two higher temperature cases, see Fig. 3. The calculated n values for these cases are shown in Fig. 10, wherein it is seen that to the same depths n values are less than those in the bulk. This is the result of two effects. First, because of the larger band gap of $\mathrm{GaP}_y\mathrm{As}_{1-y}$, the solubility of the acceptor species $\mathrm{Si}_{\mathrm{As}}^{-}$ is larger than that in GaAs, leading to a larger degree of electrical compensation and hence a smaller n value than in GaAs. The thermal equilibrium concentration ratio of the $\mathrm{Si}_{\mathrm{As}}^{-}$ and $\mathrm{Si}_{\mathrm{Ga}}^{+}$ species is [10]

$$\frac{C^{\mathrm{eq}}_{\mathrm{Si}_{\mathrm{As}}^{-}}}{C^{\mathrm{eq}}_{\mathrm{Si}_{\mathrm{Ga}}^{+}}} = \frac{g_{\mathrm{d}}}{g_{\mathrm{a}}} \frac{C^{\mathrm{eq}}_{\mathrm{Si}_{\mathrm{As}}^{0}}}{C^{\mathrm{eq}}_{\mathrm{Si}_{\mathrm{Ga}}{}^{0}}} \exp\left(\frac{2E_{\mathrm{F}} + E_{\mathrm{c}} - E_{\mathrm{v}}}{k_{\mathrm{B}}T}\right), \tag{21}$$

where g_{d} and g_{a} are, respectively, the donor and acceptor level degeneracy factors, and $C^{\mathrm{eq}}_{\mathrm{Si}_{\mathrm{As}}^{0}}$ and $C^{\mathrm{eq}}_{\mathrm{Si}_{\mathrm{Ga}}^{0}}$ are, respectively, the solubilities of the neutral Si species on the As and Ga sublattices. With E_{F} being the same throughout the heterostructure, and with the factors g_{d}, g_{a}, $C^{\mathrm{eq}}_{\mathrm{Si}_{\mathrm{As}}^{0}}$, and $C^{\mathrm{eq}}_{\mathrm{Si}_{\mathrm{Ga}}^{0}}$ regarded to be the same in $\mathrm{GaP}_y\mathrm{As}_{1-y}$ and GaAs, (21) shows that there are more acceptor species in $\mathrm{GaP}_y\mathrm{As}_{1-y}$ than in GaAs, because $E_{\mathrm{c}} - E_{\mathrm{v}}$ is larger in $\mathrm{GaP}_y\mathrm{As}_{1-y}$ than in GaAs. Second,

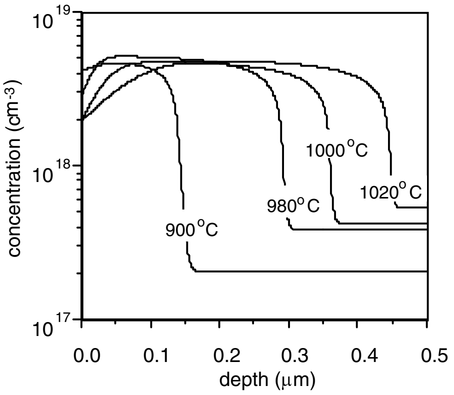

Fig. 10. Calculated electron concentration at 1000 °C in the $\mathrm{GaP}_y\mathrm{As}_{1-y}$ and GaAs P-doped Si source material case of Kavanagh et al. [2]

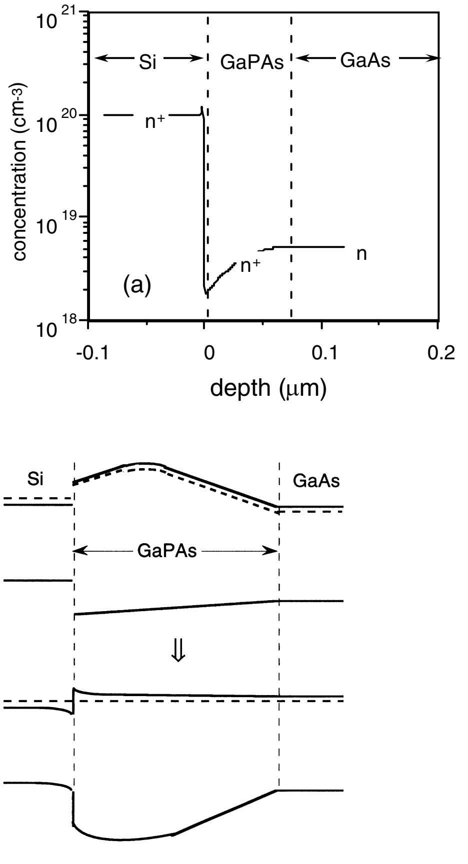

Fig. 11. **a** Calculated electron distribution at 1000 °C in Si and in III-V compounds for the P-doped Si source material case of Kavanagh et al. [2], drawn in expanded depth scale. A large electron concentration reduction in $\mathrm{GaP}_y\mathrm{As}_{1-y}$ and small electron accumulation in GaAs across the heterojunction are seen. **b** The corresponding band diagram. The *upper panel* is for the individual materials and the *lower panel* is for the same materials forming the heterostructure. The band gap of $\mathrm{GaP}_y\mathrm{As}_{1-y}$ is variable due to y variations. In the *upper panel*, the highest position of the $\mathrm{GaP}_y\mathrm{As}_{1-y}$ E_{c} curve corresponds to $y = 0.425$

there is also an electron depletion on the $\mathrm{GaP}_y\mathrm{As}_{1-y}$ side and an electron accumulation on the Si side of the heterojunction, because of the fact that E_c of $\mathrm{GaP}_y\mathrm{As}_{1-y}$ is higher than that of a separate Si crystal and that the conduction band effective density of states of $\mathrm{GaP}_y\mathrm{As}_{1-y}$ is lower than that of GaAs and much lower than that of Si. This means that in doped individual crystals the Fermi level of $\mathrm{GaP}_y\mathrm{As}_{1-y}$ is higher than that of Si and consequently in the heterostructure electrons are depleted from $\mathrm{GaP}_y\mathrm{As}_{1-y}$. For the 1000 °C case, Fig. 11a shows the electron distribution across the junction and Fig. 11b shows the corresponding band diagram. In Fig. 11a there is an electron accumulation on the Si side, but the amount is smaller than the total electron reduction on the $\mathrm{GaP}_y\mathrm{As}_{1-y}$ side for using n in the GaAs bulk as the reference value. The band diagram shown in Fig. 11b is a good illustration of the physical causes for both the higher Si self-compensation and electron depletion in $\mathrm{GaP}_y\mathrm{As}_{1-y}$. The $\mathrm{GaP}_y\mathrm{As}_{1-y}$ material possesses a graded concentration in P, with y being large at the interface and reaching 0 at a depth of $\approx 70\,\mathrm{nm}$. The reduction of electrons in GaAs surface regions decreases the effectiveness of diffusing Si into GaAs. However, this decrease appears to have been overcome by other advantages due to the use of P, which on the one hand renders the GaAs crystal to be As-rich and on the other hand the $\mathrm{Si}_\mathrm{Ga}^+$ solubility is higher.

4 Conclusions

By specifically treating the role of the Si source materials used, we have satisfactorily fitted the available experimental data on diffusing Si into GaAs. In particular, the outstanding features of the Si indiffusion profiles near the Si/GaAs interface have been quantitatively explained for the first time. Deposited on the GaAs crystal surface, the Si source material is a polycrystalline Si layer forming a heterostructure with the GaAs crystal. Without the use of an As vapor phase in the ambient, a Si source material doped by As or P effectively renders the GaAs crystal into an As-rich composition, resulting in a more efficient Si indiffusion process than for the case of using an undoped Si source material which maintains the GaAs crystal in an As-poor condition. The heterojunction influences the electron distribution in the junction region, which, in turn, affects the Si indiffusion process in the GaAs bulk. This factor is responsible for the unusual Si and electron profile features in GaAs near the Si-source/GaAs interface, particularly for the P-doped Si source cases for which $\mathrm{GaP}_y\mathrm{As}_{1-y}$ materials form.

References

1. M.E. Greiner, J.F. Gibbons: J. Appl. Phys. **44**, 750 (1984)
2. K.L. Kavanagh, C.W. Magee, J. Sheets, J.W. Mayer: J. Appl. Phys. **64**, 1845 (1988)
3. T.Y. Tan, U. Gösele: Mater. Sci. Eng. B **1**, 47 (1988)
4. S. Yu, U. Gösele, T.Y. Tan: J. Appl. Phys. **66**, 2952 (1989)
5. D.G. Deppe, N. Holonyak, Jr.: J. Appl. Phys. **64**, R93 (1988)
6. T.Y. Tan, U. Gösele: Appl. Phys. Lett. **52**, 1240 (1988)
7. H.-M. You, U. Gösele, T.Y. Tan: J. Appl. Phys. **74**, 2461 (1993)
8. C.-H. Chen, U. Gösele, T.Y. Tan: Appl. Phys. A **68**, 9 (1999)
9. C.-H. Chen, U. Gösele, T.Y. Tan: Appl. Phys. A **68**, 19 (1999)
10. C.-H. Chen, U. Gösele, T.Y. Tan: J. Appl. Phys. (1999) to be published
11. R. Scholz, U. Gösele, O. Breitenstein, U. Egger, T.Y. Tan: In *Solid State Phenomena*, Vol. 64 (Trans Tech Publications, Switzerland 1998) p. 183
12. W. Jüngling, P. Pichler, S. Selberherr, E. Guerrero, H.W. Pötzl: IEEE Trans. Electron. Devices **ED-32**, 156 (1985)
13. F.A. Trumbore: Bell System Tech. J. **39**, 205 (1960)
14. M. Capizzi, S. Modesti, F. Martelli, A. Frova: Solid State Commun. **39**, 333 (1981)